Macromolecules

COMMUNICATION TO THE EDITOR

pubs.acs.org/Macromolecules

Influence of Intermolecular Interactions on the Observable Porosity in Intrinsically Microporous Polymers

Jens Weber,*[,†] Naiying Du,[‡] and Michael D. Guiver[‡,§]

[†]Department of Colloid Chemistry, Max Planck Institute of Colloids and Interfaces, Research Campus Golm, D-14424 Potsdam, Germany

[‡]Institute for Chemical Process and Environmental Technology, National Research Council of Canada, Ottawa, Ontario K1A 0R6, Canada

[§]WCU Department of Energy Engineering, Hanyang University, Seoul 133-791, South Korea

Supporting Information

INTRODUCTION

Polymers of intrinsic microporosity (PIMs) have received significant attention during recent years, as the number of purely organic, solution-processable microporous materials continues to increase.[1−7] PIMs might be regarded as polymers of ultrahigh free volume with interconnected and accessible free-volume elements (FVE).[8] As the FVEs are accessible for probe molecules such as nitrogen, the materials can also be considered to be microporous according to IUPAC definitions.[9]

PIMs are based on a molecular design of the polymer structure, typically comprising stiff and rigid ladderlike polymer chains, which feature a contorted center or kink, e.g., a spirocenter, in each repeating unit. The rigid contorted chains pack space inefficiently, resulting in high free volume, i.e. microporosity, remaining.

The question, to which extent the porosity of intrinsically microporous polymers is determined by the molecular structure of the polymer chain, is a very tempting one. A better understanding of acting forces may enable one to anticipitate the porosity of a target structure. Recently, it was suggested that intermolecular interactions, such as hydrogen bonding, could lead to reduced or inaccessible microporosity. In some cases, this suggestion was based on observations of polymers with different linkages throughout the polymer backbone (polyamide vs polyimide).[1,10] It was not possible to completely determine whether the difference in porosity was due to interactions or if it was due to different flexibilities of the polymer backbone. A recent article also points out that residual solvents like chloroform can interact by, for example, hydrogen bonding, and the resulting structural changes can give rise to significant changes in the permeability behavior.[11]

Recently, Du et al. prepared carboxylated PIM by partial hydrolysis of the nitrile groups of PIM-1.[12] This approach has the advantage that the molecular structure of the polymer backbone is unaffected, while the amount of intermolecular interactions, i.e., the number of carboxyl groups throughout the polymer, can be adjusted (Scheme 1). Consequently, it is possible to analyze the impact of hydrogen bonding on the observable porosity while the effect of polymer flexibility can be considered as a constant.

It was shown that the gas permeability in carboxylated samples decreased with increasing degrees of hydrolysis. This suggests that the porosity of the polymers is indeed affected by the presence of the carboxylic acids.

Here we present a study of the intrinsic microporosity of such films by means of gas sorption using nitrogen and carbon dioxide as probe molecules. X-ray scattering is used additionally in order to get a better insight into the polymer microstructure. First, we investigate the "as hydrolyzed" films in detail. Second, some of the samples were dissolved and precipitated or recast. These samples were also analyzed by gas sorption in order to draw more general conclusions on the effect of intermolecular interactions.

EXPERIMENTAL SECTION

The carboxylated polymer films were prepared according to a reported protocol.[12] Gas sorption measurements were performed using an Autosorb-1 MP machine from Quantachrome Instruments. Data analysis was performed using the AS1Win Software from Quantachrome Instruments. High-purity gases were used for analysis. The polymers were degassed under high vacuum ($<10^{-7}$ bar) at 100 °C for 24 h prior to measurement. PSDs were calculated with a moving point average of 2. Measurement of film samples were undertaken after cutting the films into smaller pieces.

X-ray scattering experiments were performed using a NONIUS rotating anode instrument (4 kW, Cu Kα) with pinhole collimation and a MARCCD detector (pixel size = 79), which was calibrated using silver behenate. The distance between the sample and detector was 33.8 cm, covering a range of the scattering vector $q = 4\pi\lambda^{-1}\sin(\theta)$ from 0.65 to 8.9 nm^{-1} (2θ: scattering angle; $\lambda = 0.154$ nm). The observed scattering patterns were corrected for empty-beam scattering. The 2D diffraction patterns were transformed into a 1D radial average of the scattering intensity using the Fit2D software.

Received: June 30, 2010
Revised: March 17, 2011
Published: March 21, 2011

Scheme 1. Representative Chemical Structure of Hydrolyzed PIM-1

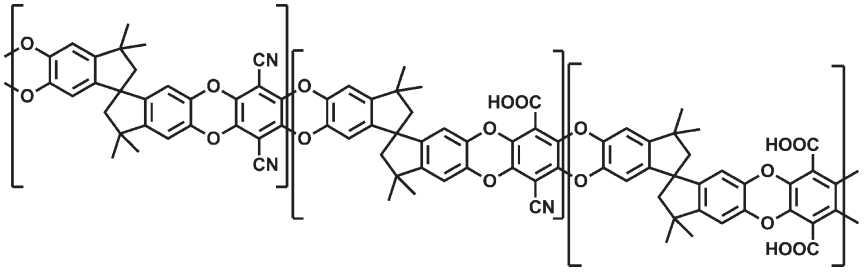

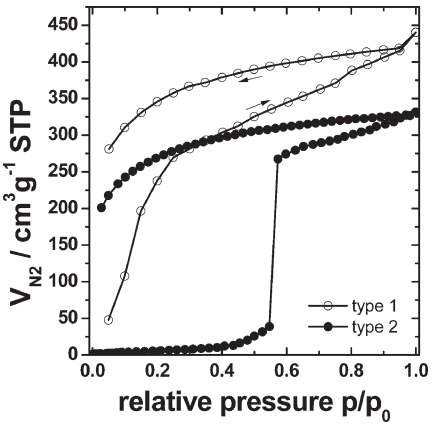

Figure 1. Typical N_2 adsorption/desorption isotherms of a PIM-1 film (measured at 77 K).

RESULTS AND DISCUSSION

Sample Preparation. PIM-1 membranes were prepared by solution casting of 1−2 wt % solution of PIM-1 (M_n = 45 kg/mol, PDI = 2.0) in chloroform. Carboxylated samples were prepared by treating the membranes with a solution of sodium hydroxide in water/ethanol, followed by neutralization and washing steps. The sample designation suffixes 1H, 3H, and 5H refer to the hydrolysis time the PIM-1 films were subjected to. The degree of hydrolysis (DH) was calculated based on FTIR measurments and elemental analysis. PIM1-1H has a DH of 11%, PIM1-3H has a DH of 64%, and PIM1-5H is fully hydrolyzed (DH ∼ 100%). After the analysis of the so-called "as-made" or "as-hydrolyzed" samples, some of the films were dissolved (PIM-1 in THF, PIM1-3H, and PIM1-5H in DMF). The polymers were either precipitated by dripping the solutions into methanol to obtain powders, or films were obtained by solution casting.

Gas Sorption. Initially, nitrogen sorption experiments were undertaken on as made PIM-1 and PIM1-1H. No observable porosity could be found for films of PIM1-1H. For PIM-1, microporosity was observed. However, different measurements on various PIM-1 film samples yielded different isotherms (Figure 1). Generally, the measurements were very slow, and it is known that nitrogen sorption on ultramicroporous samples (pores <0.8 nm) can underestimate the porosity and are sometimes affected by kinetic effects.[13−16] We observed two types of isotherms. In the first type, we found a strong uptake of N_2 even at low pressures, as typically observed for microporous materials. However, the uptake did not reach a plateau, which suggests that swelling of the polymer matrix occurs. Upon desorption, a large hysteresis was observed down to very low pressures. This is also indicative of swelling/trapping effects. The second observed isotherm type showed some gating pressure effect. No significant uptake was observed at low pressures, but at a certain point, a strong uptake took place. Upon desorption we observed again a large hysteresis. As the nitrogen sorption isotherms were inconsistent, we did not analyze them in greater detail.

It has already been suggested that other probe molecules, which do not suffer from the described kinetic effect, might be used for the analysis of ultramicroporous materials. The sorption of carbon dioxide at 273 K is well developed for the analysis of microporous carbons.[17,13−15] Its utility for the analysis of microporous polymers was already shown,[18−20] but no detailed analysis of the obtained data was performed so far. The advantage of CO_2 sorption is faster measurement times due to the higher kinetic energy of CO_2 at 273 K compared to N_2 at 77 K. The CO_2 adsorption/desorption isotherms can be analyzed by applying data evaluation methods based on NLDFT (nonlinear density functional theory) or GCMC (grand-canonical Monte Carlo) models.[17,13] Doing so, it is possible to calculate micropore size distributions (PSD) as well as specific surface areas. It should be noted that the models assume carbon materials possessing slit pores. This is certainly not perfectly true for the present materials. Nevertheless, the obtained PSDs can still give a reasonable estimate of the microporosity. Figure 2 shows the observed isotherms and the obtained PSDs.

The highest uptake of CO_2 is found for the unmodified PIM-1. Modified polymers show a slightly lower uptake; the lowest uptake is found for the fully carboxylated PIM1-5H. While for PIM-1 and PIM1-1H no hysteresis is observed upon CO_2 desorption, a small but significant hysteresis is observed for PIM1-5H. This can either be interpreted as a trapping effect due to interactions of CO_2 with the polymer or due to structural rearrangements. Comparsion of the bare adsorption isotherms (see Supporting Information for logarithmic plot) reveals that PIM-1 does adsorb less CO_2 at low pressures compared to the hydrolyzed samples PIM1-1H and PIM1-3H. At higher pressures, the isotherms cross, indicating that PIM-1 has larger pores, which gets filled at somewhat higher pressures.

Comparison of the obtained PSDs, by NLDFT as well as by GCMC, also indicates a slight decrease of the average pore size with increasing degree of hydrolysis of the nitrile groups. For PIM-1, the peak with the highest intensity is found at larger pore radii (∼2.8 nm) compared to the hydrolyzed PIM samples (e.g., PIM1-5H: ∼ 2.4−2.5 nm). This finding is consistent with the observation that no N_2 can enter the pore system already at low degree of hydrolysis. However, the PSDs should not be overestimated, and more detailed investigations must be done to

dx.doi.org/10.1021/ma101447h |*Macromolecules* 2011, 44, 1763–1767

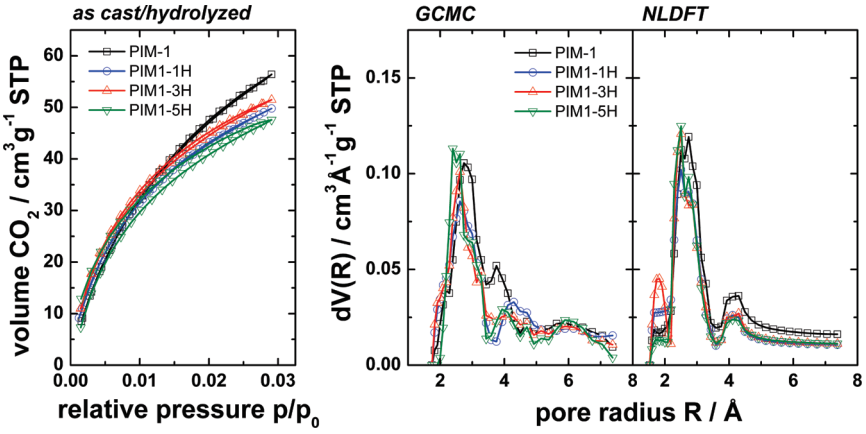

Figure 2. Left-hand side: CO_2 sorption isotherms of the as made/hydrolyzed films (measured at 273.15 K). Middle: PSDs obtained by the GCMC method. Right-hand side: PSDs obtained by the NLDFT method.

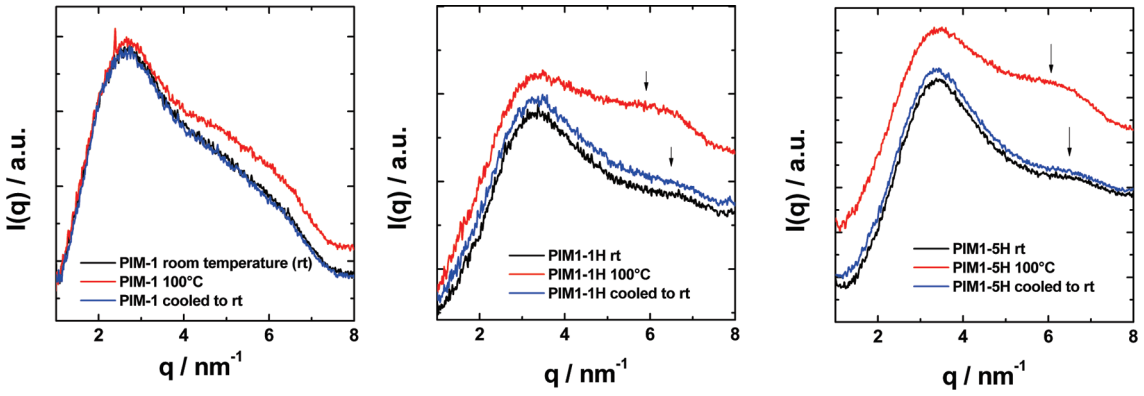

Figure 3. SAXS patterns of samples PIM-1 (left-hand side), PIM1-1H (middle), and PIM1-5H (right-hand side). The membranes were initially measured at room temperature (rt), then at 100 °C, and again after cooling to room temperature.

resolve this problem. Nevertheless, the obtained PSDs generally agree well with an independently reported PSD of PIM-1 (mean pore radius ~0.35 nm) which was determined by means of CO_2 sorption at 303 K.[21] The pore volume as determined from integration of the obtained PSDs drops from 0.195 $cm^3\ g^{-1}$ for PIM-1 to ~0.17 $cm^3\ g^{-1}$ for PIM1-1H and PIM1-3H and down to ~0.155 $cm^3\ g^{-1}$ for PIM1-5H. Generally speaking, the results obtained by analysis of the PSD correlate well with the observed decrease of permeability with increasing degree of hydrolysis.[12]

A calculation of the film density using the known skeletal density ρ_{sk} of PIM-1 (ρ_{sk} = 1.4 g cm^{-3}),[8] and the measured pore volume of 0.195 $cm^3\ g^{-1}$, results in a bulk density of $\rho \sim 1.1$ g cm^{-3}. This value compares well with reported values for PIM-1, which ranges from 1.06 to 1.12 g cm^{-3}.[8,22] Hence, it can be concluded that carbon dioxide is effective as a probe molecule for the whole accessible free volume.

As the polymer backbone, i.e., the polymer chain stiffness, is not affected by the degree of hydrolysis, it can be assumed that the reduction of the size of the free-volume elements (micropores) is due to chain deformations. It seems likely that hydrogen-bonding interactions between carboxylic acids are responsible for the observed effect. The energy gain of establishing hydrogen bonds might balance the energy, which is needed to enable the necessary deformations. Hydrogen bonds are relatively weak bonds, and it is expected that they can be broken thermally. If they are broken, it can be expected that the polymer chains will relax back into the undeformed state.

In order to check this working hypothesis, SAXS measurements of the as-made/hydrolyzed polymer films were collected at room temperature and at 100 °C, respectively. Patterns were collected in a scattering vector range between $1 < q < 8$ nm^{-1}, thus covering real space between 6.3 and 0.8 nm (Figure 3).

The patterns exhibited typically one well-defined peak at low q and a shoulder/second peak at higher q values. The first peak is found at $q = 2.65$ nm^{-1} for PIM-1 and at $q \sim 3.3$–3.4 nm^{-1} for carboxylated PIMs. The position of this peak, which can probably be related to spatial correlations between the FVEs,[23] is not influenced by a change in temperature from 25 to 100 °C. Its position also only depends on whether there are carboxylic acid groups present, but not on their quantity. Generally, the shift to larger q values upon carboxylation could be correlated to the decrease of FVE size as observed also by CO_2 sorption.

Of more interest is a qualitative analysis of the shoulder/peak, which is observed between $4.5 < q < 7$ nm^{-1}. This peak corresponds to real space sizes between 0.9 and 1.2 nm and shows a temperature response. For PIM-1, almost no influence of the temperature on the SAXS pattern is found. As the polymer is in the glassy state at both temperatures, no dramatic change of the morphology is expected.

Scheme 2. Representation of the Microstructural and Hydrogen-Bonding Changes of PIM1 upon Carboxylation[a]

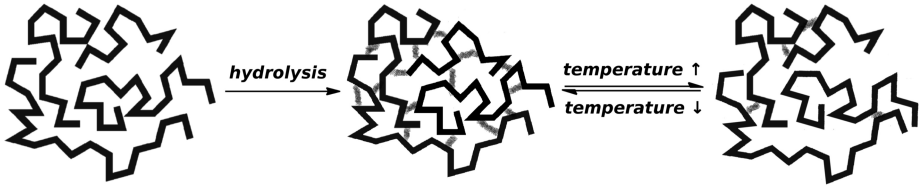

[a] Unmodified PIM-1 (left-hand side) undergoes reduction of free volume upon carboxylation due to the formation of hydrogen bonds (dashed lines). With elevated temperature, some or all hydrogen bonds can be broken, resulting in a more open morphology (right-hand side). This process is reversible upon decrease of temperature.

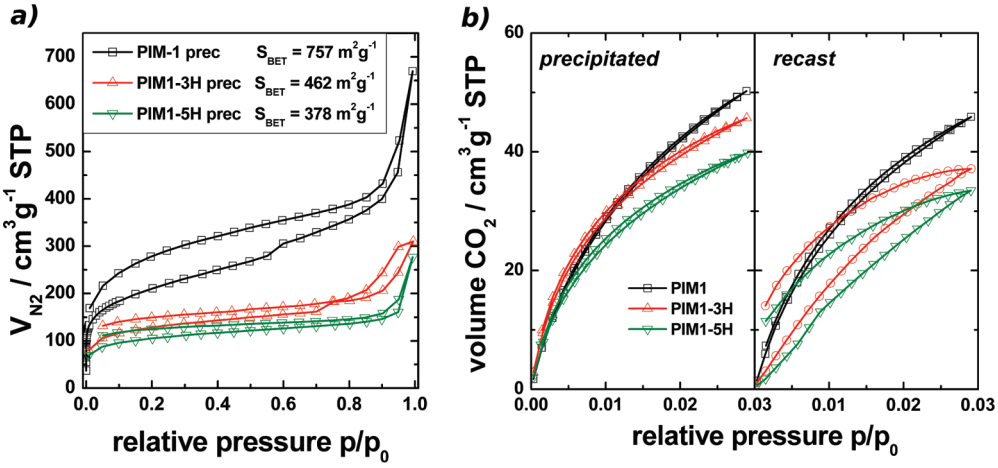

Figure 4. (a) N_2 physisorption isotherms (77 K) and apparent BET surface areas of the precipitated polymers. (b) CO_2 physisorption isotherms (273 K) of the precipitated and recast polymer films.

The situtation is different for carboxylated PIMs, although they are also in the glassy state. Here, the intensity of the second peak in relation to to the first peak increases strongly upon temperature increase. Furthermore, its position shifts toward smaller q values, which can be interpreted as an increase of the size of the FVEs. This would be in agreement with the proposed model. Upon cooling to room temperature, the SAXS pattern is the same as observed before the temperature increase. This can be interpreted as a reversible change between a (partly) relaxed morphology at high temperature and a denser, hydrogen-bonded morphology at room temperature. On the basis of these experiments, we believe that it is possible to extend the schematic picture drawn in previous publications (Scheme 2).[10,12] Carboxylation of PIM-1 leads to the establishment of inter- and intramolecular hydrogen bonds, which reduce the permeability and pore size of the polymers. At elevated temperature, some (or all) hydrogen bonds are broken, which presumably leads to an increase in FVE size.

The above-discussed results are based on investigation of the "as-hydrolyzed" films. This implies that the average chain arrangement is dictated by the original PIM-1 film, as no annealing steps were undertaken on the hydrolyzed films. In order to analyze the impact of the carboxylic acid groups in more detail, some films were dissolved and reprecipitated or recast from solution. It is known that precipitation results in a metastable state, which often possess a higher porosity and/or accessibility of the pores.[18] Therefore, we also measured the N_2 sorption isotherms of the precipitated powders. All investigated materials (PIM-1, PIM1-3H, and PIM1-5H) showed significant microporosity (see Figure 4a). Decreasing porosity was found with increasing degree of hydrolysis, in agreement with the proposed model. A micropore analysis could however only be performed on PIM-1 (see Figure S3). All attempts to measure the micropore regime of PIM1-3H or PIM1-5H by N_2 adsorption were hampered by very slow kinetics. All isotherms showed furthermore a significant low-pressure hysteresis, which is a common feature of microporous polymers. Consequently, no further characteristics apart from the apparent BET surface areas were determined (see Figure 4a).

CO_2 physisorption measurements on the precipitated samples yielded isotherms that were comparable to those obtained from the initial samples. Again, a higher uptake of CO_2 at low pressures was found for PIM1-3H compared to PIM-1, indicating again that PIM-1 possesses larger pore sizes. The PSDs were obtained by the NLDFT and GCMC method and showed the same trend as the PSDs of the original materials. (Figure S5).

Finally, the materials were solution cast again. PIM-1 was cast from THF and showed comparable characteristics as the initial sample. A slightly smaller CO_2 uptake was found (Figure 4b), which can be explained by the different solvent used for the casting. It is well-known that the solvent used for film casting can influence the permeability behavior strongly.[24] More drastic changes were observed in the case of hydrolyzed PIM1-3H and PIM1-5H, which were solution cast from DMF. The overall CO_2 uptake was smaller than for the precipitated samples, but more importantly, a large hysteresis upon desorption was observed for

those two samples. The presence of this hysteresis points to a much denser structure compared to the initial samples. Consequently, the CO_2 diffusion is limited, and no PSD is derived from those isotherms. We make the assumption that chemical interactions are not responsible for the hysteresis as such effects were absent even in the fully hydrolyzed initial membrane.

In summary, the effect of intermolecular interactions on the observable porosity in PIM-1 was investigated employing gas sorption and small-angle X-ray scattering. Hydrolysis of the side chain nitrile groups under well-defined conditions allowed the control over the amount of carboxylation. This system therefore enabled an investigation of the intermolecular interactions component only, while the polymer backbone flexibility and morphology was unchanged.

While the unmodified PIM-1 exhibited microporosity as determined by nitrogen sorption at 77 K, PIM1s modified with carboxylic acid groups did not take up nitrogen, except they were precipitated from solution. Analysis of the polymer films by carbon dioxide sorption at 273 K revealed, however, that they are also microporous. Generally, the porosity decreased when the amount of carboxylation was increased. The pore size also appears to decrease as the films are hydrolyzed, but more investigations are needed to clarify this in full detail. These findings are supported by SAXS measurements, although a thorough quantitative analysis is not possible.

Temperature-dependent SAXS measurements showed furthermore that the microstructure of the carboxylated polymer films was changed upon heating; i.e., the size of the scattering elements (FVEs) increased upon heating. This can be regarded as indirect proof of the influence of intermolecular interactions on intrinsic microporosity.

The results of the study are of interest for the development of new polymers of intrinsic microporosity. If pronounced microporosity should be achieved, it is not the simple requirement that only a rigid and kinked backbone is needed, but a reduction of potential interaction sites (such as amides, acids, etc.) must also be considered. The observation of morphological changes of the carboxylated membranes upon heating and cooling might be also of interest for potential applications such as gas separation membranes. It could for instance be envisaged that membrane permeability might be switched significantly by changing the temperature. The investigation of these effects should deserve further investigation in future studies.

■ ASSOCIATED CONTENT

Supporting Information. Further analytical data (membrane preparation details, IR data, further gas sorption data). This material is available free of charge via the Internet at http://pubs.acs.org.

■ AUTHOR INFORMATION

Corresponding Author

*E-mail jens.weber@mpikg.mpg.de; Ph ++49-331-5679569, Fax ++49-331-5679502.

■ ACKNOWLEDGMENT

Dr. Matthias Thommes (Quantachrome Instruments) is highly acknowledged for helpful discussion on the CO_2 sorption isotherms. J.W. acknowledges financial support from the Max Planck Society (EnerChem project). N.D. and M.D.G. acknowledge partial support by the Climate Change Technology and Innovation Initiative, Greenhouse Gas project (CCTII, GHG). M.D.G. acknowledges partial support from the WCU program through the National Research Foundation of Korea funded by the Ministry of Education, Science and Technology (No. R31-2008-000-10092-0).

■ REFERENCES

(1) Weber, J.; Su, O.; Antonietti, M.; Thomas, A. *Macromol. Rapid Commun.* **2007**, *28*, 1871–1876.
(2) Budd, P. M.; Ghanem, B. S.; Makhseed, S.; McKeown, N. B.; Msayib, K. J.; Tattershall, C. E. *Chem. Commun.* **2004**, 230–231.
(3) McKeown, N. B.; Budd, P. M. *Chem. Soc. Rev.* **2006**, *35*, 675–683.
(4) Du, N.; Robertson, G.; Song, J.; Pinnau, I.; Thomas, S.; Guiver, M. *Macromolecules* **2008**, *41*, 9656–9662.
(5) Du, N.; Robertson, G.; Pinnau, I.; Thomas, S.; Guiver, M. *Macromol. Rapid Commun.* **2009**, *30*, 584–588.
(6) Ghanem, B. S.; McKeown, N. B.; Budd, P. M.; Al-Harbi, N. M.; Fritsch, D.; Heinrich, K.; Starannikova, L.; Tokarev, A.; Yampolskii, Y. *Macromolecules* **2009**, *42*, 7881–7888.
(7) Budd, P. M.; McKeown, N. B. *Polym. Chem.* **2010**, *1*, 63–68.
(8) Heuchel, M.; Fritsch, D.; Budd, P. M.; McKeown, N. B.; Hofmann, D. *J. Membr. Sci.* **2008**, *318*, 84–99.
(9) Sing, K. S. W.; Everett, D. H.; Haul, R. A. W.; Moscou, L.; Pierotti, R. A.; Rouquerol, J.; Siemieniewska, T. *Pure Appl. Chem.* **1985**, *57*, 603–619.
(10) Weber, J.; Antonietti, M.; Thomas, A. *Macromolecules* **2008**, *41*, 2880–2885.
(11) Yampolskii, Y.; Alentiev, A.; Bondarenko, G.; Kostina, Y.; Heuchel, M. *Ind. Eng. Chem. Res.* **2011**10.1021/ie100097a.
(12) Du, N.; Robertson, G. P.; Song, J.; Pinnau, I.; Guiver, M. D. *Macromolecules* **2009**, *42*, 6038–6043.
(13) Vishnyakov, A.; Ravikovitch, P. I.; Neimark, A. V. *Langmuir* **1999**, *15*, 8736–8742.
(14) Jagiello, J.; Thommes, M. *Carbon* **2004**, *42*, 1227–1232.
(15) Lozano-Castelló, D.; Cazorla-Amorós, D.; Linares-Solano, A. *Carbon* **2004**, *42*, 1233–1242.
(16) The films were cut to fit into the sample tubes and should therefore have been opened to the outside.
(17) Ravikovitch, P. I.; Vishnyakov, A.; Russo, R.; Neimark, A. V. *Langmuir* **2000**, *16*, 2311–2320.
(18) Ritter, N.; Antonietti, M.; Thomas, A.; Senkovska, I.; Kaskel, S.; Weber, J. *Macromolecules* **2009**, *42*, 8017.
(19) Farha, O. K.; Spokoyny, A. M.; Hauser, B. G.; Bae, Y.; Brown, S. E.; Snurr, R. Q.; Mirkin, C. A.; Hupp, J. T. *Chem. Mater.* **2009**, *21*, 3033–3035.
(20) Weber, J.; Schmidt, J.; Thomas, A.; Böhlmann, W. *Langmuir* **2010**, *26*, 15650–15656.
(21) McKeown, N. B.; Budd, P. M. *Macromolecules* **2010**, *43*, 5163–5176.
(22) Staiger, C. L.; Pas, S. J.; Hill, A. J.; Cornelius, C. J. *Chem. Mater.* **2008**, *20*, 2606–2608.
(23) Park, H. B.; Jung, C. H.; Lee, Y. M.; Hill, A. J.; Pas, S. J.; Mudie, S. T.; Van Wagner, E.; Freeman, B. D.; Cookson, D. J. *Science* **2007**, *318*, 254–258.
(24) Budd, P. M.; McKeown, N. B.; Ghanem, B. S.; Msayib, K. J.; Fritsch, D.; Starannikova, L.; Belov, N.; Sanfirova, O.; Yampolskii, Y.; Shantarovich, V. *J. Membr. Sci.* **2008**, *325*, 851–860.